Penerbit Akademia Baru

Journal of Advanced Research Design

Journal homepage:
https://akademiabaru.com/submit/index.php/ard
ISSN: 2289-7984

Analysis Study of Fast Dynamic Response for Three-Phase Voltage Source Inverter

Noor Aqilah Madzlan[1], Noor Syafawati Ahmad[1,*], Ahmad Afif Nazib[1], Leong Jenn Hwai[1], Yaow-Ming Chen[2]

[1] Faculty of Electrical Engineering & Technology, Universiti Malaysia Perlis, Campus Alam UniMAP, Pauh Putra, 02600 Arau, Perlis, Malaysia
[2] Department of Electrical Engineering, National Taiwan University (NTU), Taipei 10617, Taiwan

ARTICLE INFO

Article history:
Received 2 March 2024
Received in revised form 28 September 2024
Accepted 4 November 2024
Available online 30 November 2024

Keywords:

Three-phase inverter; voltage source inverter (VSI); control scheme; current control; fast dynamic response

ABSTRACT

The power inverter is a crucial device employed within power grids to convert direct current (DC) into alternating current (AC). In the context of high-power grid-connected photovoltaic (PV) power generation systems, three-phase inverters have demonstrated superiority over their single-phase counterparts. Specifically, a three-phase voltage source inverter (VSI) is employed for this application. The VSI operates with a consistent input voltage while ensuring that the output voltage remains unaffected by changes in the load. However, the conventional three-phase VSI has a notable drawback. Continuous voltage and current monitoring in each phase are required to maintain synchronous operation between the power inverter and the PV-power generation system. The conventional synchronous checking procedure is relatively complex, which affects the inverter's dynamic performance. Checking for synchronisation takes time and pushes the inverter to use a more advanced controller. This sophisticated controller is crucial to evaluate the control algorithm's performance using the dynamic operation. To address these challenges, a current control strategy has been integrated into this project by implementing the synchronous reference frame current control (SRFCC) method with the proportional-integral (PI) controller. Furthermore, a synchronous reference frame phase-locked loop (SRF-PLL) is implemented in grid phase synchronisation to maintain a high-quality regulated current output. The effectiveness of this controller has been evaluated through simulations conducted using the PSIM software, providing insights into its operational behaviours and effectiveness within the project's context. According to the results obtained, it has been identified that the current control strategy with the three-phase grid-connected VSI that has been implemented in this paper is a fast dynamic response compared to the conventional inverter. The fast dynamic response inverter can reduce as much as 7.5% of the time required by the injected current to change from half-rated current to full-rated current and 2.5% of the time required by the injected current to change from full-rated current to half-rated current.

* *Corresponding author.*
E-mail address: syafawati@unimap.edu.my

https://doi.org/10.37934/ard.122.1.208218

1. Introduction

The last three decades have been marked by an increased interest in renewable energy sources (RES) since it is an unlimited source of energy, as highlighted by Ananda *et al.,* [1] Distributed generation (DG) systems need power electronic interfacing to realize grid integration and utilize renewable energy.

The main function of power electronics is to convert the voltage from DC to AC by elevating the DC input voltage to a suitable level of AC voltage with a specific predetermined frequency and magnitude. Power electronics serve a crucial role in the integration of renewable energy sources into the grid. Integrating renewable energy helps cut back on using fossil fuels, reducing harmful greenhouse gas emissions that harm the environment. Solar photovoltaic (PV) energy, biomass, wind, and hydro-energy are some of the applications of renewable energy, as discussed by Khan *et al.,* [2] and by Yu *et al.,* [3]. As for grid-connected PV systems, inverters are needed as interfaces between the PV panel and the grid. PV panels are used to convert solar irradiation into direct current while inverters are used to convert DC to AC, as conducted by Monteiro *et al.,* [4].

Through a comparison made between the single-phase inverter and the three-phase inverter, it is observed that the three-phase inverter offers a simpler control strategy and the basic topology of three-phase VSI is shown in Figure 1 from the previous study conducted by Afshari *et al.,* [5] and by Mozaffari *et al.,* [6].

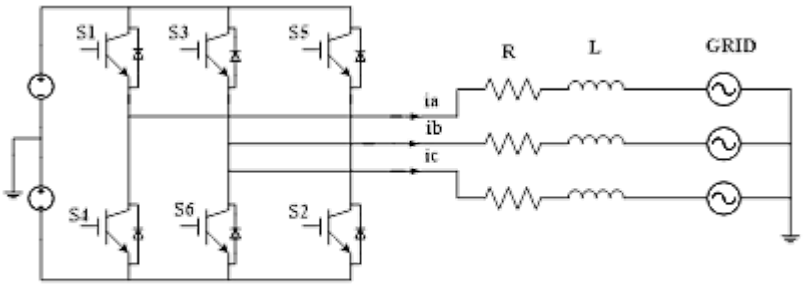

Fig. 1. Grid-connected three-phase VSI topology

In three-phase VSI, output current quality is crucial since it is one of the highest qualities. To produce a high-quality current, the characteristics of the controller used to control the output current need to be emphasised since the performance of VSI is highly dependent on the type of controller used to control its output. This is because the conventional controller for three-phase VSI requires a long calculation to tune a signal back to the power switch if there is a change in the grid voltage, as shown in Figure 2.

The value of the current that has been injected into the grid will change accordingly due to the changing grid voltage to ensure the rated power remains the same since the inverter operates at the set value of the rated power. Eren *et al.,* [7] points out in a three-phase VSI is controlled through a grid-side controller dedicated to meeting the power demands of the grid and controlling the quality of the injected current. The main emphasis of this paper is on the current control strategy, which involves fast dynamic operation. The current control strategy consists of three methods, which are natural reference frame current control, stationary reference frame current control, and synchronous reference frame current control, that is taken from the previous study [8-11].

This paper investigates the performance of the control strategy approach for three-phase grid-connected VSI by utilizing a PI current controller to obtain a fast dynamic response. The PI current controller is the best controller to be implemented in this paper among the other controllers since PI

controllers are used to avoid large disturbances during the operation process and make the system become more stable by reducing the steady-state error, as discussed by Huba *et al.,* [12] and by Dogruer *et al.,* [13]. Furthermore, the PI controller usually follows a sinusoidal reference with steady-state error due to the dynamics of the integral term stated by Cherifi *et al.,* [14]. Particularly, attention will be directed towards implementing the SRFCC method. According to the Deepthi *et al.,* [15], the SRFCC method is preferred because, during synchronization, it effectively responds to significant voltage changes and counters fast dynamics. Furthermore, an accurate grid phase synchronization is introduced to maintain a high-quality regulated current output, and the chosen approach for this grid phase synchronization is SRF-PLL. PLL is introduced to sense the grid voltage and establish a robust system capable of effectively rejecting disturbances, as introduced by Shuvo *et al.,* [16]. Simulation verifications through PSIM software confirm the fast dynamic responses of the approach current control strategy for three-phase VSI.

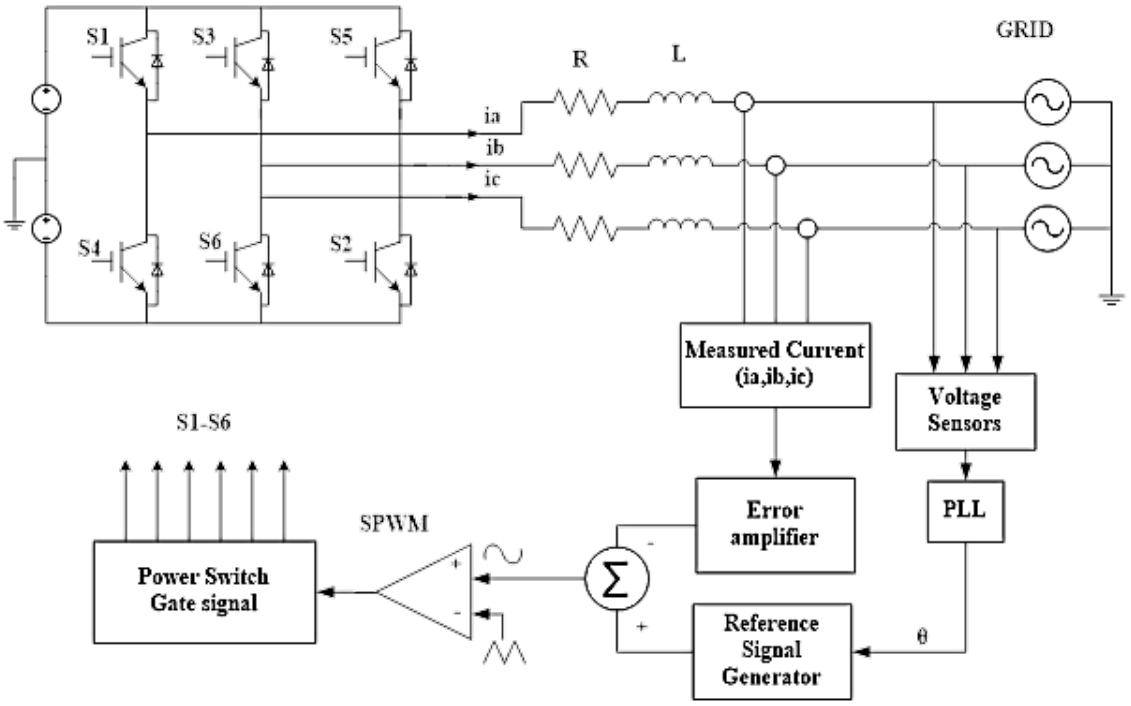

Fig. 2. Block diagram of conventional current control strategy three-phase grid-connected VSI

2. Methodology

Figure 3 shows the block diagram of the current control strategy approach for a three-phase grid-connected VSI, which consists of a three-phase VSI passed through an inductive (L) filter and into the grid, while Table 1 shows the system parameters. This filter is the simplest form of filter structure, and it is free of resonance issues compared to the higher-order filters, as discussed by Yang *et al.,* [17]. The measured current of the system is compared against a current reference, and the error between the two signals is then passed through a PI controller fed into a pulse width modulation (PWM) to generate the switching pulses based on the commanded current. Meanwhile, the PWM modulator control strategy generates the varying reference voltage modulation command and is then added and compared against the carrier signal to produce the switching pulses for the VSI, as detailed by Rusli *et al.,* [18] and Asker and Heybet [19].

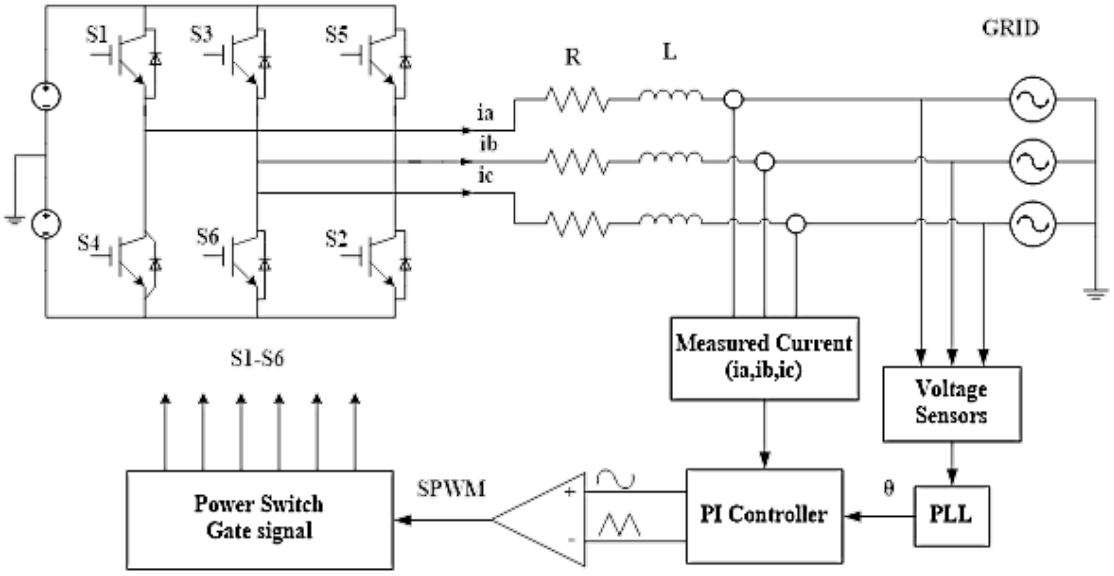

Fig. 3. Block diagram of current control strategy approach for three-phase grid-connected VSI

Table 1
System parameters

Parameter	Value
DC link voltage, V_{DC}	$700\ V$
Grid voltage, V_{ac}	$230\ V_{rms}$
Rated power, $\boldsymbol{P_{rated}}$	$5kVA$
Rated current, $\boldsymbol{I_{rated}}$	$10A$
Inductor, $\boldsymbol{L}$	$15mH$
Frequency, $\boldsymbol{f}$	$50Hz$
Switching frequency, $\boldsymbol{f_{sw}}$	$10\ kHz$
Sampling frequency, $\boldsymbol{f_{samp}}$	$20\ kHz$
Phase margin, $\boldsymbol{\emptyset_m}$	$50°$

2.1 Current Control Structure for the Three-Phase Grid-Connected VSI

In the grid-connected inverter operates as a current-controlled source to generate an output current based on a reference current signal. The current regulation algorithm regulates how much of the intended output power is delivered to the utility. The current regulation algorithm's precision is crucial for efficient maximum power processing. The effectiveness of the current regulatory algorithm is also crucial to achieving the overall harmonic distortion constraints specified by the relevant standards.

As mentioned in the literature review, numerous control methods have been developed to control inverter output current for utility-interactive operations. The linear PI controller is more suited for the grid-connected inverter application because it provides outstanding steady-state responsiveness, zero steady-state error, low current ripple, and a highly sinusoidal waveform. Since the technique does not require system models, the controller is also insensitive to system parameters. Figure 4 shows the block diagram of the control system with the PI controller. In the PI controller, to obtain a synchronous control, the feedback variables are converted into the (dq) reference frame, which is obtained by using the Park transformations. The three-phase currents and voltages from (abc) frame is transformed into (dq) frame currents and voltages. The output signals from PI controllers after dq/abc transformations are used as input to a PWM block to generate gating pulses.

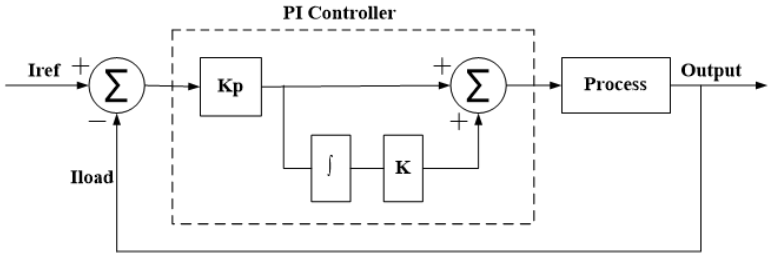

Fig. 4. Block diagram of the control system with PI controller

In this paper, two identical conventional PI controllers are used, and each of them consists of two parameters, which are proportional gain, $K_p$and integral gain, K_i. Tuning is the process of determining the optimal gains for K_p and K_i to obtain the ideal response from a control system. The PI is tuned using a variety of techniques. These parameters can be determined by using the Ziegler-Nichol's method and the equation of the parameters, which are the transfer function ($G_c(s)$), proportional gain (K_p) and integral gain (K_i), delay (T_d), and cut-off frequency (w_c) are expressed in the Eq. (1) to Eq. (3), as stated in [20]. The transfer function of PI's current controller transfer function $G_c(s)$, can be written as:

$$G_c(s) = K_p(1 + \frac{K_i}{s}) \tag{1}$$

$$K_p = \frac{w_c * L}{V_{DC}} \tag{2}$$

$$K_i = \frac{1}{(\frac{10}{w_c})} \tag{3}$$

where $w_c$is the maximum current regulator bandwidth based on the desired phase margin, $\emptyset_m$, and the delay, T_d given by Eq. (4).

$$w_c = \frac{(\frac{\pi}{2}) - \emptyset_m}{T_d} \tag{4}$$

The asymmetrical regular sampled PWM introduces a quarter-period sampling delay ZOH into the control process. The computation delay and synchronous sampling cause a further half-carrier transport delay. Therefore, the overall delay of 0.75 of the carrier periods is introduced into the forward path of the control loop.

$$T_d = \frac{0.75}{f_{sw}} \tag{5}$$

2.2 PLL Synchronisation for the Three-Phase Grid-Connected VSI

Accurate grid phase synchronisation is paramount for all grid-connected inverters to ensure precise synchronisation with the grid and maintain a high-quality regulated current output. Achieving this synchronisation is commonly facilitated by utilising a PLL mechanism. The primary objective of the PLL is to sense the grid voltage and establish a robust system capable of effectively rejecting disturbances. This ensures accurate estimation of the grid phase angle, even when confronted with challenging scenarios of grid distortion. Within the framework of this study, the chosen approach for

grid phase synchronisation is the SRF-PLL. This widely recognised method employs a Parks transform to convert the intricate three-phase voltages into distinct direct and quadrature DC voltage components.

At its core, the SRF-PLL consists of a phase detector (PD) that takes on the dual form of a Clarke transform, and a Park transform. These integral components work harmoniously to extract essential information from the grid voltage. This is a loop filter intricately integrated with a PI loop controller. This amalgamation serves the crucial purpose of refining the quadrature DC voltage signal, represented as v_q. The primary role of the PI controller is to regulate the quadrature voltage signal precisely, v_q, in a manner that nullifies phase errors. The PI controller ensures accurate grid phase synchronisation through its carefully crafted control mechanism by maintaining precise alignment with the grid voltage.

In essence, the SRF-PLL serves as the cornerstone for achieving meticulous grid phase synchronisation. By adeptly combining elements like the Clarke and Park transforms with the precision of the PI loop controller, this mechanism effectively addresses disturbances and enables accurate phase angle estimation, even amidst challenging circumstances of grid distortion. Eq. (6) shows the transfer function of the PLL.

$$LF\ (s) = \ k_{PLL}\left(\frac{1+k_{iPLL}}{s}\right) \tag{6}$$

where k_{PLL} is the PLL proportional gain and k_{i_PLL} is the PLL integral gain. These gains are computed for this work using the symmetrical optimal method that was explored by Golestan *et al.,* [21] where the proportional gain, k_{PLL} and the integral gain, k_{i_PLL} is calculated using the Eq. (7) and Eq. (8):

$$k_{PLL} = 2\pi f_c \tag{7}$$

$$k_{i\_PLL} = \frac{k_{PLL}}{g} \tag{8}$$

The parameter f_c denotes the cut-off frequency, a pivotal factor that determines the bandwidth of the PLL. Complementing this is the coefficient g, a value that encapsulates the dynamic behaviour of the PLL when subjected to frequency and phase transients. For this study, a value of $g = 2.4$ is meticulously chosen in accordance with the methodology outlined by Golestan *et al.,* [21]. Ultimately, the output derived from the PLL controller, v_q,interfaces with a feedforward constant representing the nominal frequency. Furthermore, the integration of this frequency lends itself to the estimation of the input phase angle denoted as θ_{PLL}. This estimated phase angle then undergoes feedback into the phase detector's Park transform. The outcome of this transformation serves as the foundation for generating the sinusoidal reference, a vital component in the current regulator's operation. In summary, the interplay between the cut-off frequency, the coefficient g, and the integration of frequency estimation shapes the behaviour of the PLL. This intricate process, guided by the feedback loop, culminates in generating a sinusoidal reference pivotal for accurately operating the current regulator in the grid-connected inverter system.

3. Results

3.1 Dynamic Performance Evaluation of Current Controller

The fast dynamic response of the proposed control strategy in this paper has been investigated using a PSIM software simulation of a three-phase grid-connected VSI according to the configuration in Figure 3 and the parameters in Table 1.

Dynamic responses pertain to waveforms that manifest when a system is subjected to disturbances, with these disruptions originating from variations such as load changes, step changes, and voltage changes. The assessment of dynamic response revolves around gauging the promptness with which a controller can adapt to modifications in grid parameters. For instance, in dynamic performance, any irregularities emerging on the grid side, specifically in voltage levels, while an inverter operates, lead to the inverter's current control mechanism making necessary adjustments to uphold the stipulated power output. A deliberate step change was introduced in the current reference under normal operational conditions to analyse the dynamic response in this experimental context. This step change facilitated an assessment of how effectively the system could acclimate to sudden modifications and highlighted the controller's agility in maintaining optimal performance.

Below, Figure 5 portrays the output voltage waveform of a three-phase VSI across its constituent phases: phase a, phase b, and phase c. This measurement is taken at the inverter's output. Furthermore, Figure 6 shows the output current waveform for each phase. According to the waveform shown in Figures 5 and 6, it appears to be a normal condition where the inverter operates in a balanced mode. Consequently, the voltage and current waveforms are balanced across the three phases (a, b, and c).

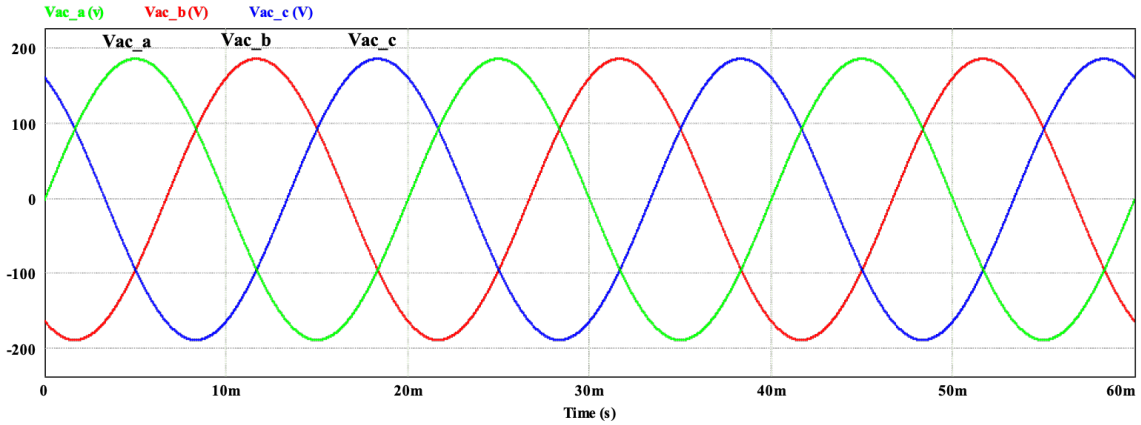

Fig. 5. Output voltage waveform of three-phase VSI for each phase

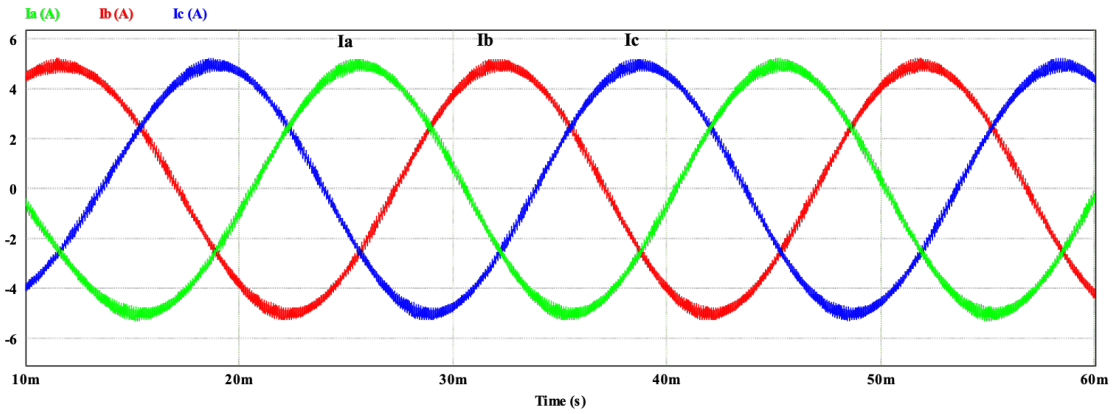

Fig. 6. Output current waveform for each phase

Moving on to Figure 7 and Figure 8 below, it presents the response of the controller to an injected current, (i_d), reference current, $(i_{d(ref)})$ and error current, $\left(i_{d(err)}\right)$ with step changes for both conventional inverter and fast dynamic inverter. As for the waveforms in Figure 7 and Figure 8, both inverters initially operate at half of their rated current, starting at 5 A. Subsequently, at 20 ms, both inverters receive commands to operate at their full rated current, increasing from 5 A to 10 A. At 40 ms, a command is issued to the inverters to return to half the rated current, reducing from 10 A to 5 A. These figures offer insight into the behaviour of the VSI's output current as it responds to these changes in reference. The green colour waveform represents the injected current, while the red colour waveform represents the reference current.

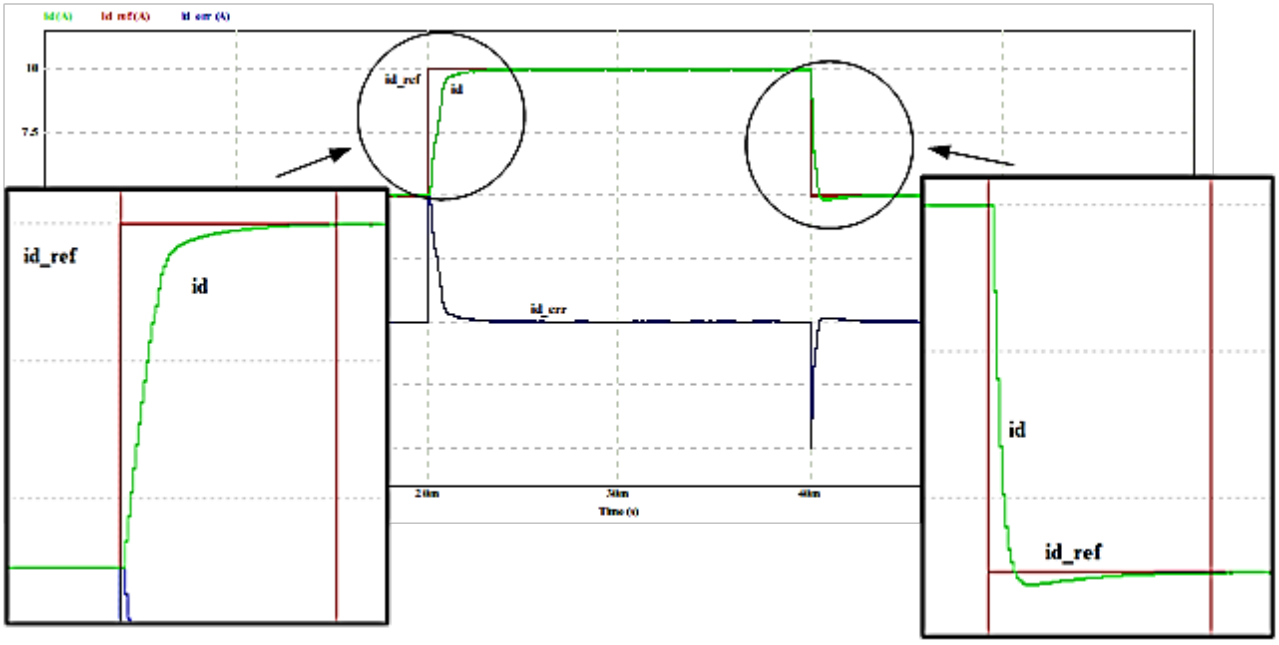

Fig. 7. The waveform of injected current, (i_d), reference current, $(i_{d\ (ref)})$and error current, $\left(i_{d(err)}\right)$ with step change for the conventional inverter

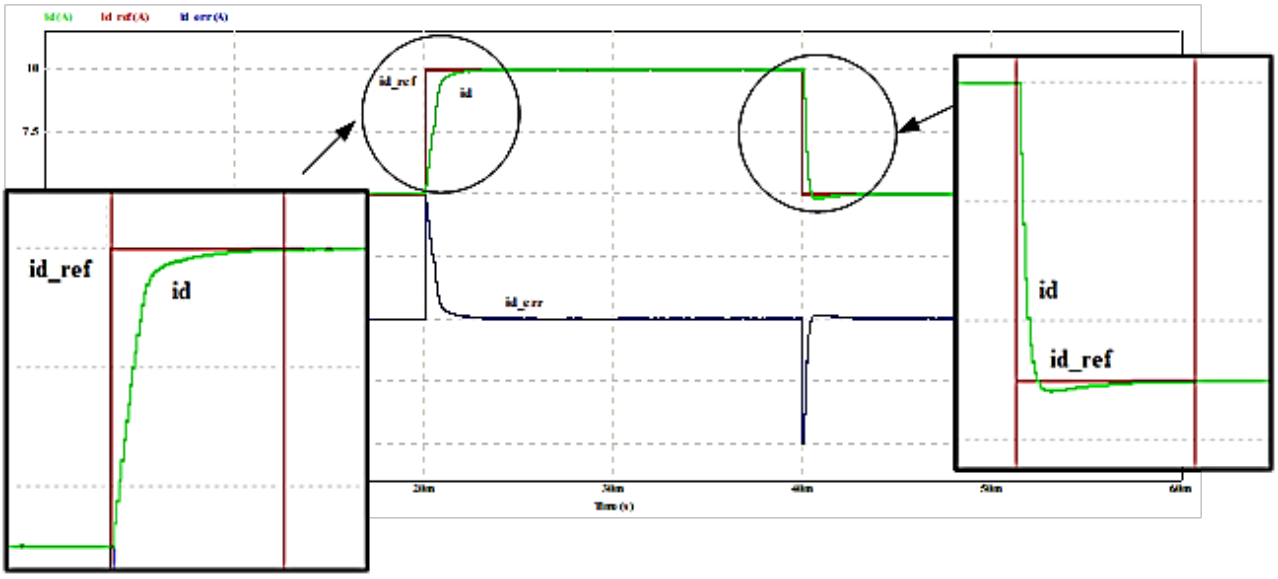

Fig. 8. The waveform of injected current, (i_d), reference current, $(i_{d\ (ref)})$and error current, $\left(i_{d(err)}\right)$ with step change for the fast dynamic inverter

A conventional inverter required 4 ms to transform from a half-rated current to a full-rated one at t=0.02s when the inverter received the command. It can be shown in Figure 7 in the box on the left side. From full-rated to half-rated current, it required 3.9 ms, as seen in the box on the right side of Figure 7. Next, for the fast dynamic inverter, the transformation from half-rated current to full-rated current is accomplished within 3.7 ms, as shown in the box on the life side of Figure 8. Moving to the box on the right side of Figure 8 required 3.8 ms to transform from a full-rated current to a half-rated one.

Next, Figure 9 and Figure 10 depict the output current waveforms of each respective phase for the conventional inverter and the fast dynamic inverter, respectively, with step changes. According to Figure 9 and Figure 10, this appears to be a normal condition in which the inverter operates in a balanced mode, with the current waveforms across the three phases (a, b, and c) balanced for both conventional and fast dynamic inverters with step changes.

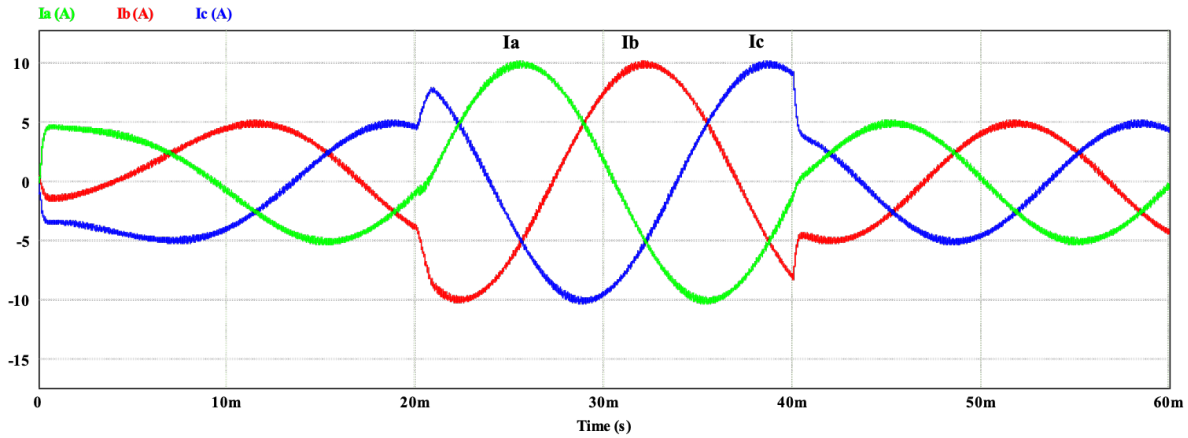

Fig. 9. Output current waveform of each phase with step changes for the conventional inverter

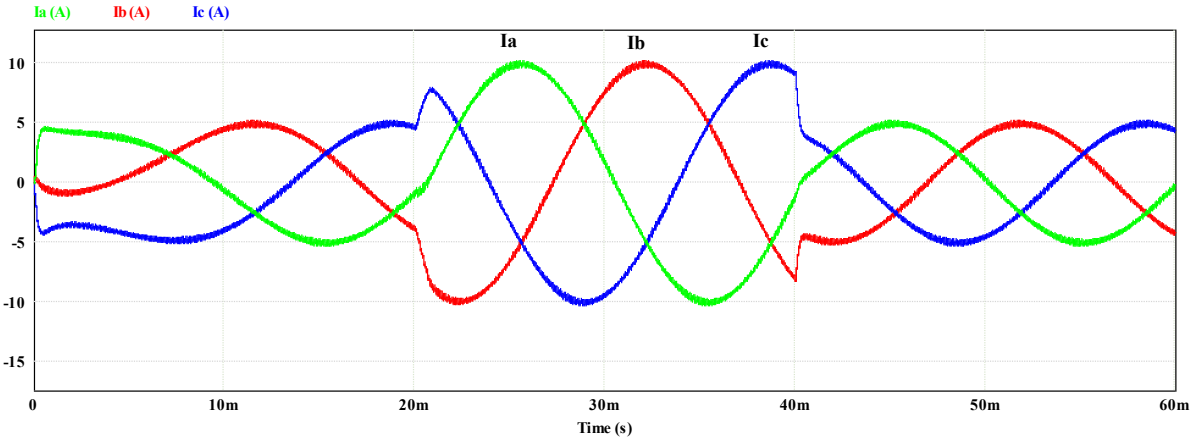

Fig. 10. Output current waveform of each phase with step changes for the fast dynamic inverter

4. Conclusions

This paper presents the fast dynamic response of a three-phase grid-connected VSI with a current control strategy. The performance of the control strategy has been validated using simulation. According to the results obtained, it has been identified that the current control strategy with the three-phase grid-connected VSI that has been implemented in this paper is a fast dynamic response compared to the conventional inverter. Based on Figure 7 and Figure 8, it is revealed that the fast

dynamic inverter can reduce as much as 7.5% of the time required by the injected current to change from half-rated current, 5 A, to full-rated current, 10 A, according to the instructions given by the step-up change in the reference current. Next, during step-down change, the fast dynamic inverter can decrease the time needed for the injected current to shift from the full rated current of 10 A to half the rated current of 5 A by 2.5%. The control strategy is verified using PSIM software simulation of a three-phase VSI, achieving a fast dynamic response.

Acknowledgement
The authors would like to thank and greatly appreciate all the people who have supported to preparing this paper. The authors would like to acknowledge the support from the Fundamental Research Grant Scheme (FRGS) under the grant number FRGS/1/2021/TK0/UNIMAP/03/1.

References

[1] Ananda-Rao, Kumuthawathe, Afifah Shuhada Rosmi, Steven Taniselass, Nor Hanisah Baharudin, Mafizah Hamid, Leow Wai Zhe, and Suresh Kumar Sudabattula. "MPPT charge controller using fuzzy logic for battery integrated with solar photovoltaic system." *Journal of Advanced Research in Applied Sciences and Engineering Technology* 47, no. 2 (2024): 171-182. https://doi.org/10.37934/araset.47.2.171182

[2] Khan, Md Noman H., Mojtaba Forouzesh, Yam P. Siwakoti, Li Li, Tamas Kerekes, and Frede Blaabjerg. "Transformerless inverter topologies for single-phase photovoltaic systems: A comparative review." *IEEE Journal of Emerging and Selected Topics in Power Electronics* 8, no. 1 (2019): 805-835. https://doi.org/10.1109/JESTPE.2019.2908672

[3] Yu, Zhixiang, Xuefeng Hu, Meng Zhang, Lezhu Chen, and Shunde Jiang. "A transformerless boost inverter for stand-alone photovoltaic generation systems." In 2019 IEEE 10th international symposium on power electronics for distributed generation systems (PEDG), p. 570-575. IEEE, 2019. https://doi.org/10.1109/PEDG.2019.8807688

[4] Monteiro, Filipe, Eduardo Sarquis, and Paulo Branco. "Identifying critical failures in PV systems based on PV inverters' monitoring unit: A techno-economic analysis." *Energies* 17, no. 18 (2024): 4738. https://doi.org/10.3390/en17184738

[5] Afshari, Ehsan, Gholam Reza Moradi, Ramin Rahimi, Babak Farhangi, Yongheng Yang, Frede Blaabjerg, and Shahrokh Farhangi. "Control strategy for three-phase grid-connected PV inverters enabling current limitation under unbalanced faults." *IEEE Transactions on Industrial Electronics* 64, no. 11 (2017): 8908-8918. https://doi.org/10.1109/TIE.2017.2733481

[6] Mozaffari, Khalegh, Mahshid Amirabadi, and Yateendra Deshpande. "A single-phase inverter/rectifier topology with suppressed double-frequency ripple." *IEEE Transactions on Power Electronics* 33, no. 11 (2018): 9282-9295. https://doi.org/10.1109/TPEL.2018.2797125

[7] Eren, Suzan, Alireza Bakhshai, and Praveen Jain. "Control of three-phase voltage source inverter for renewable energy applications." *In 2011 IEEE 33rd International Telecommunications Energy Conference (INTELEC)*, p. 1-4. IEEE, 2011. https://doi.org/10.1109/INTLEC.2011.6099761

[8] Briz del Blanco, Fernando, and Marko Hinkkanen. "Design, implementation and performance of synchronous current regulators for AC Drives." *Chinese Journal of Electrical Engineering*, 4 (2018). https://doi.org/10.23919/CJEE.2018.8471290

[9] Roy, Suchismita, Pradeep Kumar Sahu, and Satyaranjan Jena. "Analysis and control strategy of standalone PV system with various reference frames." *Open Engineering* 12, no. 1 (2022): 616-626. https://doi.org/10.1515/eng-2022-0371

[10] Roy, Suchismita, Pradeep Kumar Sahu, Satyaranjan Jena, and Amiya Kumar Naik. "Feedback current control techniques for a single-phase grid-connected photovoltaic system." In *2022 2nd Odisha International Conference on Electrical Power Engineering, Communication and Computing Technology (ODICON),* p. 1-6. IEEE, 2022. https://doi.org/10.1109/ODICON54453.2022.10010141

[11] Hisar, Cagdas, Ibrahim Sefa, and Necmi Altin. "Fixed-frequency sliding mode control in synchronous reference frame for three-phase LCL filtered active front-end converter." In *2022 IEEE 20th International Power Electronics and Motion Control Conference (PEMC)*, p. 295-300. IEEE, 2022. https://doi.org/10.1109/PEMC51159.2022.9962883

[12] Huba, Mikulas, Stefan Chamraz, Pavol Bistak, and Damir Vrancic. "Making the PI and PID controller tuning inspired by Ziegler and Nichols precise and reliable." *Sensors* 21, no. 18 (2021): 6157. https://doi.org/10.3390/s21186157

[13] Dogruer, Tufan, and Nusret Tan. "Design of PI controller using optimization method in fractional order control systems." *IFAC-PapersOnLine* 51, no. 4 (2018): 841-846. https://doi.org/10.1016/j.ifacol.2018.06.124
[14] Cherifi, Abdelhafid, Aissa Chouder, Abdelhalim Kessal, Abdelhak Hadjkaddour, Ali Aillane, and Kalil Louassaa. "Control of a voltage source inverter in a microgrid architecture using PI and PR controllers." In *2022 19th International Multi-Conference on Systems, Signals & Devices (SSD)*, p. 1471-1477. IEEE, 2022. https://doi.org/10.1109/SSD54932.2022.9955891
[15] Deepthi, V., and B. A. Sridhara. "Implementation of synchronous reference frame theory based pwm generation for dc to ac conversion." *International Journal of Engineering Research Technology (IJERT)* 4, no. 5 (2015): 1388-1391. https://doi.org/10.17577/IJERTV4IS051229
[16] Shuvo, Shuvangkar, Eklas Hossain, and Ziaur Rahman Khan. "Fixed point implementation of grid tied inverter in digital signal processing controller." *IEEE Access* 8 (2020): 89215-89227. https://doi.org/10.1109/ACCESS.2020.2993985
[17] Yang, Yugang, Lei Wang, and Heming Sun. "A design of PWM inverter passive filter based on CM transformer." *CPSS Transactions on Power Electronics and Applications* 5, no. 2 (2020): 180-190. https://doi.org/10.24295/CPSSTPEA.2020.00015
[18] Rusli, Muhammad Rizani, Mochamad Ari Bagus Nugroho, Mentari Putri Jati, Angga Wahyu Aditya, Melinda Badriatul Fauziah, Handri Toar, and Taufik Taufik. "Digital implementation of space vector PWM for three phase inverter with simplified C-Block PSIM utilization." In *2021 International Electronics Symposium (IES)*, p. 24-29. IEEE, 2021. https://doi.org/10.1109/IES53407.2021.9593292
[19] Asker, Mehmet Emin, and Heybet Kilic. "Modulation index and switching frequency effect on symmetric regular sampled SPWM." *European Journal of Technique (EJT)* 7, no. 2 (2017): 102-109. https://doi.org/10.23884/ejt.2017.7.2.04
[20] Ahmad, Noor Syafawati, Noor Aqilah Madzlan, Ahmad Afif Nazib, and Leong Jenn Hwai. "Accurate simplified SPWM control strategy for single-phase voltage source inverter under varying grid conditions." In *2023 IEEE Conference on Energy Conversion (CENCON)*, p. 150-154. IEEE, 2023. https://doi.org/10.1109/CENCON58932.2023.10368685
[21] Golestan, Saeed, Mohammad Monfared, and Francisco D. Freijedo. "Design-oriented study of advanced synchronous reference frame phase-locked loops." *IEEE Transactions on Power Electronics* 28, no. 2 (2012): 765-778. https://doi.org/10.1109/TPEL.2012.2204276